






## Article

# Accurate Analytical Model and Evaluation of Wi-Fi Halow Based IoT Networks under a Rayleigh-Fading Channel with Capture

Hamid Taramit <sup>1,2,\*</sup> , Jose Jaime Camacho-Escoto <sup>3</sup> , Javier Gomez <sup>4</sup> , Luis Orozco-Barbosa <sup>2</sup>   
and Abdelkrim Haqiq <sup>1</sup> 

- <sup>1</sup> Computer, Networks, Mobility and Modeling Laboratory (IR2M), Faculty of Sciences and Techniques, Hassan First University of Settat, Settat 26000, Morocco; abdelkrim.haqiq@uhp.ac.ma
- <sup>2</sup> Albacete Research Institute of Informatics, Universidad de Castilla-La Mancha, 02006 Albacete, Spain; luis.orocho@uclm.es
- <sup>3</sup> Faculty of Engineering, National Autonomous University of Mexico, Mexico City 04510, Mexico; jcamachoe@comunidad.unam.mx
- <sup>4</sup> Department of Telecommunications Engineering, National Autonomous University of Mexico, Mexico City 04510, Mexico; javiergo@comunidad.unam.mx
- \* Correspondence: h.taramit@uhp.ac.ma



**Citation:** Taramit, H.; Camacho-Escoto, J.J.; Gomez, J.; Orozco-Barbosa, L.; Haqiq, A. Accurate Analytical Model and Evaluation of Wi-Fi Halow Based IoT Networks under a Rayleigh-Fading Channel with Capture. *Mathematics* **2022**, *10*, 952. <https://doi.org/10.3390/math10060952>

Academic Editors: Daniel-Ioan Curiac and Pedro A. Castillo Valdivieso

Received: 2 February 2022

Accepted: 12 March 2022

Published: 16 March 2022

**Publisher's Note:** MDPI stays neutral with regard to jurisdictional claims in published maps and institutional affiliations.



**Copyright:** © 2022 by the authors. Licensee MDPI, Basel, Switzerland. This article is an open access article distributed under the terms and conditions of the Creative Commons Attribution (CC BY) license (<https://creativecommons.org/licenses/by/4.0/>).

**Abstract:** The IEEE 802.11ah standard, marketed as Wi-Fi Halow, introduces a new channel access mechanism called the Restricted Access Window (RAW), aiming to provide connectivity for the Internet of Things (IoT) applications over broad areas. RAW aspires to alleviate the contention by splitting the channel access into periods and allocating each period to a given group of stations. This paper develops an analytical framework based on Probability and Renewal theories for modeling and evaluating an IEEE 802.11ah-based network implementing the RAW mechanism. We consider a Rayleigh-fading channel with the presence of the capture effect: a realistic scenario for IoT networks deployed in dense urban environments. Considering a single-hop scenario of stations randomly distributed around an Access Point (AP) and the power attenuation of transmitted packets, we model the channel access under capture awareness. As the RAW mechanism presents a time-limited contention for channel access, we develop a counting process that tracks transmissions up to the end of the contention time interval. Henceforth, we evaluate the network performance in terms of throughput. We meticulously validate the derived analytical results through extensive campaigns of discrete-event simulations. Our study evaluates the impact of different parameters on the overall performance, including the contention time, the number of stations, the number of groups, and the capture threshold. We henceforth study the impact of the capture effect on enhancing the network performance under the grouping feature introduced by the RAW mechanism. This work contributes to developing an analytical modeling framework to evaluate the performance of time-limited random access mechanisms accurately and can be an excellent basis for proposing practical scheduling algorithms to configure the RAW mechanism under non-ideal channel conditions.

**Keywords:** performance evaluation; renewal theory; stochastic process; IEEE 802.11ah; RAW mechanism; capture effect; Internet of things

**MSC:** 60K05; 68M20

## 1. Introduction

The Internet of Things (IoT) has evolved into an essential paradigm that brings significant changes to human life where connectivity is available anywhere, anytime for anything [1]. As IoT incorporates an increasing number of devices, it is vital to develop wireless communication technologies that meet the requirements of IoT applications, such

as large-scale connectivity, low power consumption, and reliable throughput [2]. It is anticipated that new wireless technologies will ensure a reliable interconnection of a massive number of IoT devices, such as sensors, smartphones, and home appliances. Two types of low-power IoT communication technologies are currently available: Wireless Personal Area Network (WPAN) and Low-Power Wide Area Network (LPWAN) technologies [3]. WPAN technologies (e.g., Zig-Bee and Bluetooth) provide medium data rates (i.e., up to a few hundred kilobits per second) at short range (i.e., tens of meters), whereas LPWAN technologies (e.g., LoRa and SigFox) provide long-range communications (i.e., up to tens of kilometers) at low data rate (i.e., up to a few kilobits per second). As such, it is still required to have an IoT communication technology offering higher data rates.

Since its invention, Wi-Fi technology has established a great success becoming one of the most commonly utilized wireless technologies globally. However, with the emergence of the IoT, the requirements for wireless connectivity have shifted tremendously. The traditional Wi-Fi technology is not applicable for IoT scenarios, as it is designed only for small-scale networks with a few dozen stations over a small range of tens of meters. Therefore, the IEEE Task Group ah (TGah) developed the IEEE 802.11ah standard [4], the first Wi-Fi solution to address IoT applications and fill the gap between existing low-power IoT communication technologies. The IEEE 802.11ah Wi-Fi standard was officially released in 2016, presenting several amendments to the legacy Wi-Fi technology. It operates in unlicensed sub-1GHz frequency bands, and it supports the connectivity of up to 8192 stations with a single Access Point (AP). In addition, it provides data rates ranging from 150 Kbps to 78 Mbps over a transmission range up to 1 km [3]. IEEE 802.11ah introduces a new channel access mechanism, called Restricted Access Window (RAW), aiming to provide efficient connectivity to densely deployed, energy-constrained devices.

The RAW mechanism is based on periodic channel reservation, where only a set of stations can access the channel simultaneously. Such a feature makes the IEEE 802.11ah standard an excellent solution for long-range IoT use cases, such as smart sensors and meters, backhaul aggregation, and extended range hotspot and cellular offloading [5]. Hereafter, an IEEE 802.11ah based network can be implemented to cover thousands of widely distributed sensors and meters. It can also carry out the backhaul connection between IEEE 802.15.4g devices and their remote servers. Additionally, IEEE 802.11ah can be deployed to enlarge the hotspot range and traffic offloading in mobile networks.

The time-limited contention within short periods of RAW slots presents a new challenge to derive accurate evaluation for the overall performance of a single RAW slot or a RAW consisting of several RAW slots. The legacy analytical models based on steady-state results as Bianchi's [6] are not applicable in this case. The channel access contention within a RAW slot is terminated at the end of its period, which prevents the system from reaching the stationary state [7]. Henceforth, the RAW mechanism is critically affected by the time constraint presented by the RAW slots periods. Since the standard did not mention how to configure RAWs within beacon intervals and RAW slots within RAW, an accurate evaluation of the performance of a given configuration is necessary in order to derive efficient scheduling and configuration algorithms. However, we do not focus on RAW configuration strategies in this work. Instead, we shall develop an accurate analytical framework to evaluate the contention within a RAW slot period and a RAW consisting of several RAW slots. We assume that the RAW periods within beacon intervals are allocated in a way that eliminates the hidden nodes problem so that all stations assigned to a given RAW can listen to each other.

In addition, the role of the RAW mechanism in decreasing collisions, the Capture Effect (CE) feature imports significant enhancements to the network performance by enhancing channel usage during RAW periods. That is, when a collision occurs, the receiver can still capture the data frame from one station when its received signal exceeds that of other interfering signals by a certain threshold. Furthermore, the received signal depends on the channel model, which characterizes the wireless medium and depends on several parameters, such as the distance between the transmitter and receiver, the line of sight,

and the environment (obstacles and surroundings) [8]. We consider in this work an IEEE 802.11ah based network operating under a Rayleigh fading channel model with capture. This channel model represents a heavily built-up urban environment and a non-line-of-sight (NLOS) propagation in the wireless channel [9].

The contributions of this work are summarized as follows:

- We model the channel access within a RAW slot under a Rayleigh fading channel with capture, considering the geometric distribution of stations around the AP.
- We develop a renewal theory based framework to model the contention within the RAW slot by deploying a counting process to track transmissions within the RAW slot period. We then evaluate the RAW slot throughput representing the channel usage ratio in delivering data frames during the RAW slot period.
- We derive the throughput of a RAW consisting of several RAW slots, which represents the channel usage ratio to deliver data frames during the overall RAW duration. We also evaluate the RAW performance in a no-capture channel scenario and derive the capture ratio in a given RAW configuration.
- We present a meticulous validation of the analytical findings through extensive simulations obtained via a discrete-event simulator developed with the MATLAB software. We henceforth carry out a discussion and analysis of several parameters affecting the performance of a RAW slot and a RAW consisting of several RAW slots.

The remainder of the paper is organized as follows: Section 2 describes the RAW mechanism and reviews previous works modeling and evaluating the RAW mechanism and the capture effect. Then, in Section 3, we describe the considered scenario and the channel model. We also carry out the modeling of the channel access mechanism in the presence of capture effect and power attenuation under a Rayleigh fading channel. Section 4 presents a renewal theory based model to evaluate the RAW slot throughput, representing the channel usage ratio to deliver data frames during the RAW slot period. We henceforth derive the throughput of a RAW comprising several RAW slots and highlight the capture ratio in the RAW period. In Section 5, we validate our analytical findings via simulations and examine the impact of several parameters on the performance of a RAW slot and a RAW consisting of several RAW slots. Finally, we conclude our work in Section 6.

## 2. Background

### 2.1. The IEEE 802.11ah RAW Mechanism

Although IEEE 802.11ah inherits most of the legacy IEEE 802.11 features, several amendments have been proposed in this new standard to support the general requirements of long-distance dense IoT networks. The novel hierarchical Association Identification (AID) structure allows a single IEEE 802.11ah AP to associate up to 8191 stations. Furthermore, the IEEE 802.11ah standard operates in the unlicensed sub-1GHz frequency band and provides connectivity over a range of up to 1 km. Since connecting thousands of stations using basic IEEE 802.11 MAC mechanisms is impossible, the IEEE 802.11ah standard introduces a new MAC mechanism named Restricted Access Window (RAW).

The RAW mechanism aims to alleviate collisions and improve the performance of dense IoT networks where a significant number of devices are contending for channel access simultaneously. It can be viewed as a combination of deterministic and stochastic media access strategies. Figure 1 depicts a schematic representation of the RAW mechanism functionality. Within each beacon interval, the AP allocates one or more RAWs, where each RAW is allocated to a group of stations. During a RAW period, only its designated stations are allowed to contend for channel access. In contrast, all stations can access the channel in the shared channel time. The AP is responsible for allocating RAW periods within the beacon interval and assigning a group of stations to each RAW. Thus, it broadcasts this information through the preceding beacon frame using the RAW Parameter Set (RPS) element. The RPS element indicates the stations assigned to RAWs, the configuration of RAWs, and the starting time of each RAW.

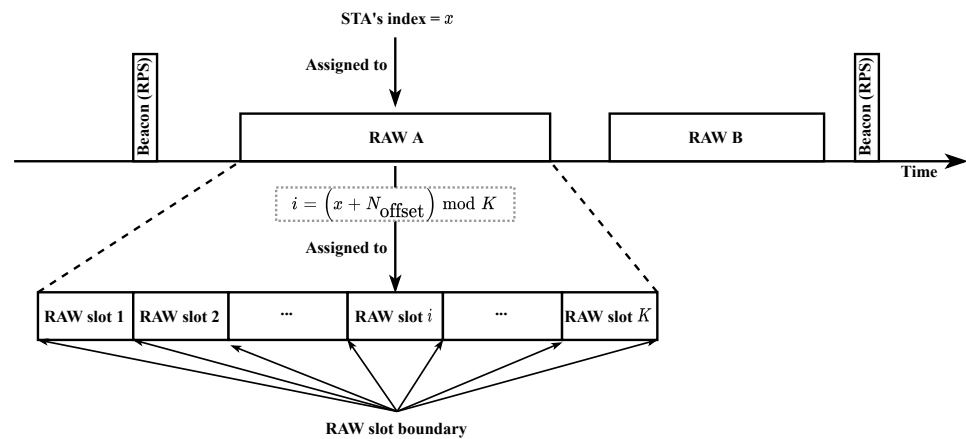


**Figure 1.** Schematic representation of the RAW mechanism.

To reduce the contention even more, each RAW can be divided into one or more short periods referred to as RAW slots, and the stations assigned to a RAW are also split across the RAW slots using a round-robin assignment policy. Each station is allowed to contend for channel access only during its designated RAW slot and prohibited from contending for medium access during the other RAW slots of the RAW. The number of RAW slots within each RAW and their duration are also included in the RPS element. A station determines the index of the RAW slot  $i_{\text{slot}}$  in which it is allowed to begin competing for medium access based on the following mapping function [4]:

$$i_{\text{slot}} = (x + N_{\text{offset}}) \bmod K, \quad (1)$$

where  $x$  is the position index of the station among others in the RAW,  $N_{\text{offset}}$  represents the offset value in the mapping function, and  $K$  is the number of RAW slots in the RAW.

During each RAW slot, assigned stations use DCF or EDCA mechanism to access the channel. To make that compatible with the RAW mechanism, each station maintains two backoff function states to manage medium access inside and outside its assigned RAW slot [4]. The first backoff function is used outside RAW slots during the shared channel time, where all stations contend for channel access, while the second is used inside. At the start of each RAW period, every station stores and suspends the state of its first backoff function, then later it restores and resumes the backoff timer at the end of the RAW period. The second backoff function is used inside RAW periods, where each station initiates the backoff timer at the beginning of its designated RAW slot, then terminates and discards the backoff timer state at the end of the RAW slot. This paper focuses on evaluating the performance inside the RAW, where the assigned stations are using only the second backoff function procedure. Hence, we do not consider the correlation of the two backoff function states.

## 2.2. Related Work

The IEEE 802.11ah standard comes with significant improvements over the legacy Wi-Fi technology, making it an excellent Wi-Fi solution for IoT applications. It is shown that the IEEE 802.11ah standard provides better performance than the other alternatives in terms of data rate, coverage range, association time, and delay [10]. The amendments in the IEEE 802.11ah standard make this new technology prominent in developing reliable IoT network infrastructures. Numerous studies have previously been conducted on the standard's key features to show the potentials and challenges in designing the new proposed mechanisms [5]. Domazetović et al. [11] evaluated the achievable range of IEEE 802.11ah based systems. Their findings demonstrated that IEEE 802.11ah standard is extremely promising for various IoT applications. Additionally, as shown in [12], implementing an IEEE 802.11ah-based infrastructure may be less expensive than a system based on the traditional IEEE 802.11 technology. Šljivo et al. [13] established a performance evaluation

of the RAW mechanism using the ns-3 network simulator. Their results show that an IEEE 802.11ah based network can connect up to 10 and 20 streaming IP-cameras with data rates of 160 kbps and 255 kbps, respectively, over a 200 m distance. The authors in [14] carried out the efficacy of the RAW mechanism in high-contention scenarios. They showed that the RAW mechanism significantly enhances the network performance in terms of throughput and energy efficiency. Furthermore, they emphasized the necessity of optimizing the RAW parameters to maximize network resource usage.

Several works carried out analytical models to evaluate IEEE 802.11ah based networks [15–18]. The authors in [17] presented an analytical framework to model the contention within a RAW slot using a four dimension Markov chain. The Markov process is defined by the number of stations and occurred slots in idle, success, and collision states. However, they did not provide any closed-form results as there are no explicit definitions of the probabilities of the absorbing states, which is the main objective of the proposed model. The same model is deployed in [15] to evaluate the energy consumption within the RAW, under the assumption that every station has only one packet to transmit in each beacon interval. In [18], the authors proposed a mathematical model for EDCA within RAW without retries, i.e., a station gets only one attempt to transmit its packet. Although such a scenario would have very limited applications, it is an easy to calculate model compared to the normal EDCA with retries as the authors depicted while comparing it with the model in [17]. A similar model with no retries is presented in [16] with an additional assumption that a RAW slot can host at most only one transmission attempt, which is an even more limited scenario for real network applications. In contrast to the aforementioned models, we propose in this paper a more sophisticated approach for modeling the contention within the RAW slot period. Our approach is based on developing a counting process that continuously tracks transmissions as arrivals on the wireless medium, while the interarrivals are presented by the preceding idle slots and the previous transmission. To the best of our knowledge, we are the first to propose this approach that is less complex in computing than the models in [15,17], as it yields closed-form results for the time-limited contention in the RAW mechanism. Additionally, we consider a non-ideal channel with capture effect enabled, which is omitted in the works mentioned above.

In real-life applications, the capture effect highly affects the network performance, and the signal of a transmitted packet is subject to fading effects over the channel, background noise, and potential interference from concurrent transmissions. An IEEE 802.11ah based IoT network in an urban environment will be affected by many factors. Considering that the coverage is up to 1 km, NLOS conditions with respect to the AP are not met for all stations. Besides, a transmitted signal in such an environment will be subject to reflections, resulting in multipath fading at the receiver. Such a scenario is mainly represented by a Rayleigh fading channel [19]. Several works carried out an analytical framework to evaluate the performance of a network operating under a Rayleigh fading channel. In [20,21], the authors presented a Markov chain model to evaluate the throughput of a DCF-based network. They considered a non-ideal channel with capture effects in a Rayleigh fading environment. Their study was carried out within saturated [21] and unsaturated [20] scenarios. Similar work was reported in [22], where the authors proposed a 3-D Markov Chain based model to evaluate a homogenous 802.11 network operating with the DCF mechanism under a Rayleigh fading channel that incorporates transmission error and capture. The analytical frameworks presented in these works have some shortcomings in the capture effect modeling. First, they do not consider the geometric distribution of stations around the AP. Second, they assume that all stations are power-controlled so that the mean received power of interfering packets is the same. Third, they compute the capture probability at the level of slot states so that when a slot contains a collision, one packet from one of all stations can still be captured. However, that may not be accurate, as only a few stations will participate in a collision at a given slot. In this work, we take these shortcomings into account besides the time-limited contention presented in the RAW mechanism. We also consider the geometric distribution of stations around the



AP and the same transmission power for all stations so that the mean received powers of interfering packets are different and depend on the distance from the AP to the source stations. Furthermore, we compute the capture probability at the level of a transmitted packet as a subevent of the packet collision. Hence, such a result is extended to derive a slot that contains collision with a capture.

During the contention in a wireless network, the timeline of a station or the wireless medium is discretely occupied by a limited number of events (e.g., successful transmissions, collisions, idle slots) occurring repeatedly. Each event occurs periodically, creating renewal cycles. Renewal theory is an adequate mathematical approach that studies similar behavior of periodic events. This approach is dedicated to processes that occur at random instants at which the system returns to a state probabilistically equivalent to the starting state [23]. The authors in [24] introduced a three-level renewal process framework, modeling the periodic channel access in the IEEE 802.15.4 standard. However, their model does not apply to the DCF MAC protocol as medium access in IEEE 802.15.4 is based on a non-persistent Carrier Sense Multiple Access (CSMA) mechanism. In [25], Zhang presented a renewal process to model the backoff procedure of a station within a non-saturated IEEE 802.11 network. The introduced method is more precise and practical than Bianchi's approach, particularly for non-saturated scenarios. In [26], the authors established a renewal theory based model to evaluate the IEEE 802.11 multichannel MAC protocol by deploying a two-level renewal process. Nevertheless, the time-limited contention factor introduced in the RAW mechanism is not considered in [25,26]. The models introduced in these works are based on renewal cycles that provide accurate results only in the case of a long enough contention time.

A renewal process can also be associated with a counting process that tracks events in terms of time. The authors in [27] introduced the simple counting processes and their extension to generalized counting processes under the presence of environmental stochasticity, where the generalization corresponds to the case in which the process transitions depend on the environmental conditions. Henceforth, in this work, we develop a counting process that tracks transmission in the medium up to a given time. Although the different events occupying the channel yield a discrete timeline, the counting process is defined in a continuous timeline, which presents a challenge to adapt such a process to a wireless medium. This process can be seen as a generalized counting process defined in [27], where the process transitions depend on the outcome of wireless medium slots. The developed counting process provides accurate modeling for the limited channel access introduced in the RAW mechanism, and to the best of our knowledge, the counting process is not deployed before in the literature to model medium access contention.

### 3. System Model

This section expounds the network system and the channel access model. First, Section 3.1 introduces the network scenario considered. Then, Section 3.2 describes the Rayleigh fading channel model. Thereafter, Section 3.3 presents the analytical model for channel access under fading and capture awareness. Finally, Section 3.4 yields the different states of a channel slot.

#### 3.1. Scenario

We consider an IEEE 802.11ah-based network consisting of stations randomly distributed over a given area around one AP within a radius  $\rho$ , as illustrated in Figure 2. We assume that the entire beacon interval is occupied by one RAW and that all stations are allocated to this RAW. Note that this RAW may contain one or more RAW slots. Our goal is to model the contention within a RAW slot, and then evaluate and analyze the performance of a single RAW slot and a RAW consisting of several RAW slots. We consider a channel with capture effect enabled, taking into account the distances of stations from the AP and the fading of transmissions throughout the channel. The AP assigns a RAW to a set of

stations that have packets to deliver. Thus, we aim to examine the gain of the RAW in the worst scenario, and therefore we consider a network with saturated traffic.

During the RAW slot period, only the assigned stations are allowed to compete for channel access using the Enhanced Distributed Channel Access (EDCA) protocol [4]. The station first checks if the channel is unoccupied for a DCF Interframe Spacing (DIFS) time. Then, it selects a random backoff time counter uniformly from  $[0, W_j - 1]$ ,  $j \in [0, m]$ , where  $W_j$  is the size of the current Contention Window (CW), and  $m$  denotes the number of backoff stages. The CW is initiated with the value  $W_0$ , and it doubles after each collision until it achieves the maximum size  $W_m = 2^m \cdot W_0$ . When the transmitted packet is delivered successfully or dropped, the CW resets to  $W_0$ . Note that the transmission attempt of a given packet can only be initiated at the beginning of the time slot, and the packet is dropped after  $m$  failed retransmissions. The station gets a transmission opportunity (TXOP) to transmit its packets when its backoff time counter reaches zero. For the convenience of analysis and to keep fair resources allocation for stations, we assume that a TXOP allows only the transmission of one packet, and its duration is given by:

$$T_{\text{TXOP}} = T_{\text{DATA}} + \text{SIFS} + T_{\text{ACK}}, \quad (2)$$

where  $T_{\text{ACK}}$  is the transmission time of an acknowledgment frame (ACK). The Short Inter-frame Space (SIFS) is the time interval between the transmission of a data frame and its corresponding ACK, defined in the standard.  $T_{\text{DATA}}$  is the transmission time of a data frame defined as follows:

$$T_{\text{DATA}} = T_{\text{PLCP}} + \frac{\text{Payload} + \text{MacHeader}}{\text{DataRate}}. \quad (3)$$

For the convenience of analysis, we assume that all stations assigned to the RAW belong to the same Access Category (AC) and carry similar fixed-size payloads.

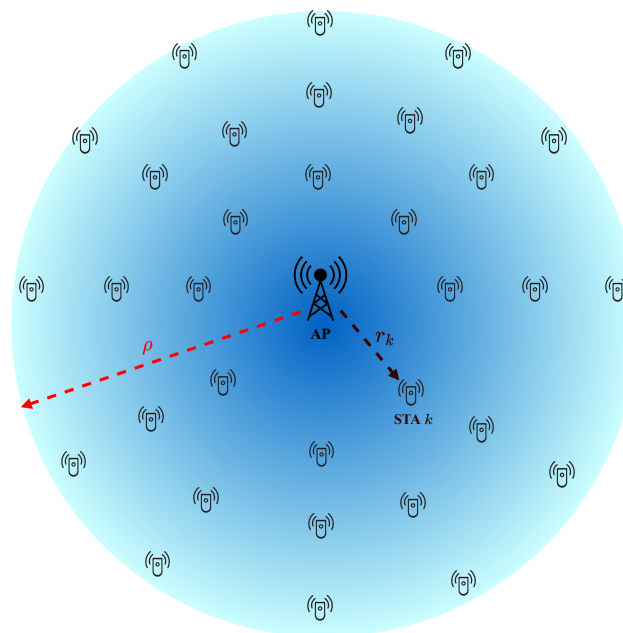


**Figure 2.** Illustration of the network scenario.

### 3.2. Channel Model

The capture effect imports significant improvements to the network performance by decoding one packet from a collision of several stations. Thus, when two stations or more transmit simultaneously, and a collision occurs, it is still possible for the AP to capture the data frame from one station if the power of its received signal exceeds that of interfering stations by a certain threshold. However, the received power of a transmitted

packet depends on the channel model representing the behavior and changes of transmitted signals throughout the channel. The channel model characterizes the wireless medium and depends on several parameters, such as the distance between the transmitter and receiver, the line of sight, and the environment (obstacles and surroundings) [8]. Therefore, the signal of a transmitted packet is subject to fading effects over the channel, background noise, and potential interference from concurrent transmissions. We omit in this paper the impact of background noise and focus only on the impact of interference and fading effects. The IEEE 802.11ah standard mainly addresses long-distance IoT use cases, where there is mostly a lack of line of sight (LOS) between stations and the AP. Henceforth, we consider a Rayleigh fading channel model representing a heavily built-up urban environment where transmissions are subject to multipath fading and NLOS propagation in the wireless channel [9].

During simultaneous transmission of  $n + 1$  stations, the packet of a tagged transmitting station  $k$  is assumed to be captured by the AP if and only if its instantaneous power  $\omega_k$  exceeds the instantaneous joint interference power  $\omega_{int} = \sum_{i=1}^n \omega_k$  by at least a threshold  $z$ . This threshold reflects the capture performance of the AP, and it is referred to as the capture threshold. Furthermore, with the consideration of a Rayleigh fading channel model, the instantaneous power of a received packet from station  $k$  is exponentially distributed as follows [28]:

$$f_{\omega_k}(x) = \frac{1}{\omega_{0k}} e^{-\frac{x}{\omega_{0k}}}, \quad x \geq 0 \quad (4)$$

where  $\omega_{0k}$  is the local mean power of the transmitted packet at the receiver, and it is defined as follows:

$$\omega_{0k} = A \cdot r_k^{-\alpha} \cdot \omega_T. \quad (5)$$

where

- $\omega_T$  is the transmitted signal power.
- $A \cdot r_k^{-\alpha}$  represents the deterministic path-loss law, where  $r_k$  is the distance between the station  $k$  and the AP.
- $\alpha$  is the path-loss exponent, and it depends on the propagation environment. For the convenience of analysis, we assume  $\alpha = 4$  for the rest of this paper.
- $A$  is a dimensionless constant in the path-loss law.

We assume that the constants  $A$  and  $\omega_T$  are the same for all transmitted packets.

### 3.3. Capture Aware Channel Access

Although there are works in the literature that model the channel access under the capture effect feature [20–22], they derive the packet capture probability as a subevent of a slot containing a collision. However, such a result is not exactly accurate as capturing a given packet is a subevent of the collision of the same packet. Henceforth, in our model, we track the packet transmitted from a tagged station and derive its capture probability conditioned to its collision. We then extend this result to obtain the probability of having a captured packet in a randomly chosen slot.

Consider a RAW slot allocated to  $N_S$  stations. In order to consider the capture effect in the channel access analysis, we assume  $N_S \geq 2$ . The case of  $N_S = 1$  presents no collisions, and hence no capture. Thus, it belongs to the scenario of no-capture channel, which we discuss later in Section 4.2.

We assume that all stations inside the RAW slot attempt to transmit packets with the same probability  $\tau$ . Let  $p$  denote the probability that the transmission attempt of a packet fails to be successfully delivered. Denote by  $A$  and  $B$  two random variables representing the attempts and backoffs experienced by a single transmitted packet, respectively. Using the mean value analysis method as in [29], we define the probability  $\tau$  as follows:

$$\tau = \frac{E[A]}{E[A] + E[B]} \quad (6)$$



where  $E[\cdot]$  is the mathematical expectation function.

Given that each packet can be retransmitted up to  $m$  times, both  $A$  and  $B$  follow a truncated geometric distribution with the rate  $p$  and different supports  $\Omega_A$  and  $\Omega_B$ , respectively. Thus, we have

$$\Omega_A = \{1, 2, \dots, m+1\},$$

and

$$\Omega_B = \left\{ \frac{W_0}{2}, \sum_{k=0}^1 \frac{2^k W_0}{2}, \dots, \sum_{k=0}^m \frac{2^k W_0}{2} \right\}.$$

Hence,

$$E[A] = \sum_{k=0}^m (k+1) \cdot \frac{(1-p)p^k}{1-p^{m+1}} = \frac{1 + (m+1)p^{m+2} - (m+2)p^{m+1}}{(1-p)(1-p^{m+1})}, \quad (7)$$

and

$$E[B] = \sum_{k=0}^m \frac{2^k W_0}{2} \cdot \frac{(1-p)p^k}{1-p^{m+1}} = \frac{W_0(1 + (1-2^{m+2}(1-p) - 2p)p^{m+1})}{2(1-2p)(1-p^{m+1})}. \quad (8)$$

Thus, we substitute (7) and (8) in (6) to obtain the probability  $\tau$  for a station to initiate the transmission its packet in a given slot expressed as follows:

$$\tau = \frac{2(2p-1)(1 + (m+1)p^{m+2} - (m+2)p^{m+1})}{W_0(1-p)((2^{m+2}-1)p^{m+1} - (2^{m+2}-2)p^{m+2} - 1) + 2(2p-1)(1 + (m+1)p^{m+2} - (m+2)p^{m+1})}. \quad (9)$$

A transmitted packet from a tagged station will encounter a collision if at least one of the remaining  $N_S - 1$  stations starts transmitting in the same time slot. Thus, the packet collision probability is defined as follows:

$$p_{col}^p = 1 - (1 - \tau)^{N_S - 1}. \quad (10)$$

Since we consider a channel with capture effect feature enabled, a packet involved in a collision may be captured and delivered successfully. Let  $p_{cap}^p$  be the probability of capturing a transmitted packet after encountering a collision. The capture of a transmitted packet is a subset event of the collision events; a tagged packet fails to be delivered if it experiences a collision and is not captured. Hence, the probability  $p$  for fail delivery of a transmitted packet is given by:

$$p = p_{col}^p \cdot (1 - p_{cap}^p). \quad (11)$$

A prior definition for the probability  $p_{cap}^p$  to capture a transmitted packet after encountering a collision is given by:

$$p_{cap}^p = \frac{\sum_{n=1}^{N_S-1} R_n \cdot \Pr\{z/n+1\}}{p_{col}^p}, \quad (12)$$

where  $\Pr\{z/n+1\}$  is the average conditional capture probability (ACCP) for  $n+1$  interfering packets. This probability is defined by the probability of signal-to-interference ratio  $\gamma = \frac{\omega_0}{\omega_{int}}$  exceeding the threshold  $z$ . We have

$$\Pr\{z/n+1\} = \Pr\{\gamma > z/n+1\}. \quad (13)$$

$R_n$  is the probability that the transmitted packet encounters  $n$  interfering packets, and it is given by:

$$R_n = \binom{N_S-1}{n} \tau^n (1-\tau)^{N_S-1-n}. \quad (14)$$

We now proceed to determine the expression of the ACCP defined in (13). This probability depends on the received powers of the captured signal and the interfering packets. Furthermore, the received power of a given packet depends on the distance of the source station from the AP.

All  $N_S$  stations are randomly distributed around the AP in a circular area of radius  $\rho$ , as illustrated in Figure 2. Hence, the Probability Density Function (PDF) of the distance between a station and the AP is given by:

$$h(r) = \frac{2r}{\rho^2}, \quad 0 \leq r \leq \rho. \quad (15)$$

Assume that the AP is receiving  $n + 1$  packets simultaneously. Among these packets, we tag one packet transmitted by a station located at a distance  $r_0$  from the AP.

Let  $\omega_{00}, \omega_{01}, \dots, \omega_{0n}$  be the local mean powers of the tagged packet and the  $n$  interfering packets, respectively. The conditional capture probability for the tagged packet can be expressed as follows:

$$\begin{aligned} Pr\{z/r_0, r_1, \dots, r_n\} &= Pr\{\gamma > z/r_0, r_1, \dots, r_n\} \\ &= Pr\left\{\omega_0 > z \cdot \sum_{i=1}^n \omega_k / r_0, r_1, \dots, r_n\right\} \\ &= \int_0^\infty f_{\omega_1}(x_1) \left( \int_0^\infty f_{\omega_2}(x_2) \cdots \int_0^\infty \left( f_{\omega_n}(x_n) \cdot \int_{z \cdot \sum_{i=1}^n \omega_k}^\infty f_{\omega_0}(x_0) dx_0 \right) dx_n \cdots dx_2 \right) dx_1 \\ &= \int_0^\infty f_{\omega_1}(x_1) \left( \int_0^\infty f_{\omega_2}(x_2) \cdots \int_0^\infty \left( f_{\omega_n}(x_n) \cdot e^{-\frac{z \cdot \sum_{i=1}^n \omega_k}{\omega_{00}}} \right) dx_n \cdots dx_2 \right) dx_1 \\ &= \frac{1}{1 + z \cdot \frac{\omega_{0n}}{\omega_{00}}} \cdot \int_0^\infty f_{\omega_1}(x_1) \left( \int_0^\infty f_{\omega_2}(x_2) \cdots \int_0^\infty \left( f_{\omega_{n-1}}(x_{n-1}) \cdot e^{-\frac{z \cdot \sum_{i=1}^{n-1} \omega_k}{\omega_{00}}} \right) dx_{n-1} \cdots dx_2 \right) dx_1 \\ &\vdots \\ &= \prod_{k=1}^n \frac{1}{1 + z \cdot \frac{\omega_{0k}}{\omega_{00}}} \\ &= \prod_{k=1}^n \frac{1}{1 + z \cdot \left( \frac{r_k}{r_0} \right)^{-4}}. \end{aligned} \quad (16)$$

Since all stations are distributed following the PDF  $h(\cdot)$  defined (15), all factors in the product in (16) are statistically equal. Consequently, the average conditional capture probability for the tagged packet when encountering  $n$  interfering packets can be defined as follows:

$$\begin{aligned} Pr\{z/r_0, n\} &= \left( \int_0^\rho \frac{h(r)}{1 + z \cdot \left( \frac{r}{r_0} \right)^{-4}} dr \right)^n \\ &= \left( 1 - \frac{r_0^2 \sqrt{z}}{\rho^2} \cdot \arctan \left( \frac{\rho^2}{r_0^2 \sqrt{z}} \right) \right)^n \end{aligned} \quad (17)$$

Given that the distance  $r_0$  is also randomly distributed following the PDF  $h(\cdot)$ , the ACCP to capture one packet from  $n + 1$  interfering packets can be derived by integrating  $Pr\{z/r_0, n\}$  over all possible values of the distance  $r_0$  from the AP. Henceforth, the ACCP  $Pr\{z/n\}$  is expressed as follows:

$$\begin{aligned} Pr\{z/n\} &= \int_0^\rho Pr\{z/r_0, n\} \cdot h(r_0) dr_0 \\ &= \int_0^\rho \left( 1 - \frac{r_0^2 \sqrt{z}}{\rho^2} \cdot \arctan \left( \frac{\rho^2}{r_0^2 \sqrt{z}} \right) \right)^n \cdot \frac{2r_0}{\rho^2} dr_0. \end{aligned} \quad (18)$$

Consequently, by substituting (14) and (18) in (12), we derive the expression of the probability  $p_{cap}^p$ . We have

$$p_{cap}^p = \frac{1}{p_{col}^p} \sum_{n=1}^{N_S-1} \binom{N_S-1}{n} \tau^n (1-\tau)^{N_S-1-n} \cdot \int_0^\rho \left( 1 - \frac{r_0^2 \sqrt{z}}{\rho^2} \cdot \arctan \left( \frac{\rho^2}{r_0^2 \sqrt{z}} \right) \right)^n \cdot \frac{2r_0}{\rho^2} dr_0. \quad (19)$$

Note that the integral in this expression can only be calculated by numerical integration.

Moreover, the values of probabilities  $\tau$ ,  $p$ , and  $p_{cap}^p$  can be obtained by resolving numerically the non-linear system defined by (9), (11) and (19).

### 3.4. Channel Slot State

During the RAW slot period, all assigned stations contend for channel access, and each station starts transmitting with probability  $\tau$ . Hence, the probability  $P_i$  that a randomly chosen slot is idle is given by:

$$P_i = (1 - \tau)^{N_S}. \quad (20)$$

The probability  $P_s$  of a packet being transmitted and successfully delivered without interference is defined as the probability to have exactly one station that transmits, conditioned on the current slot to be not empty. We have

$$P_s = \frac{N_S \cdot \tau \cdot (1 - \tau)^{N_S-1}}{1 - P_i}. \quad (21)$$

Let  $P_{cap}$  be the probability to deliver a packet successfully after being captured in a collision. Since only one packet can be captured from each collision,  $P_{cap}$  is given by the probability that one of the  $N_S$  stations transmits and its packet is captured, conditioned to the fact that the current slot contains a collision. Hence, we have

$$P_{cap} = \frac{N_S \cdot \tau \cdot p_{cap}^p}{(1 - P_i)(1 - P_s)}. \quad (22)$$

Henceforth, during the RAW slot period, the channel comprises several slots that we classify into four types. As illustrated in Figure 3, a randomly chosen slot can be in only one of the following four states:

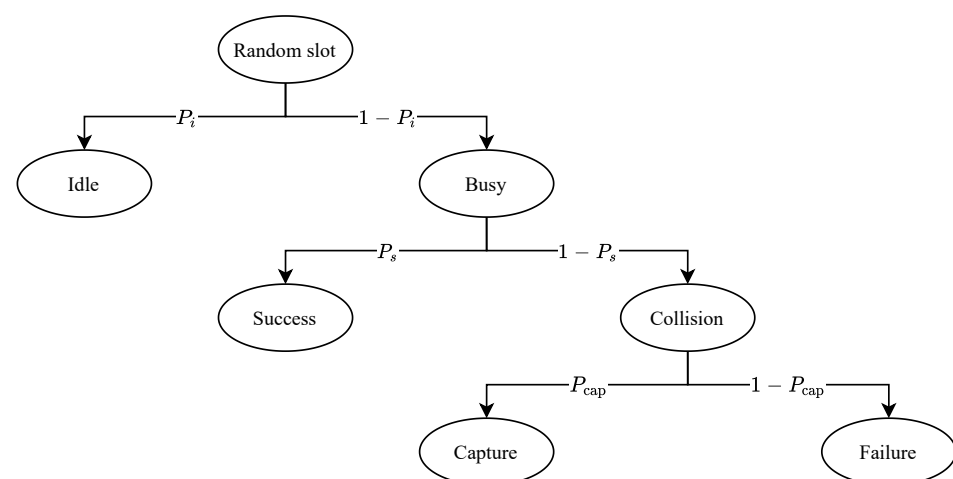


Figure 3. Different states of a randomly chosen slot.

- Idle: When there are no ongoing transmissions in the slot. That is, all stations are listening to the medium while counting down their backoff counter. A randomly chosen slot is idle with probability  $P_i$ .

- Success: When only one station transmits and its packet is delivered successfully. Given that this state is a subset of busy slots, a randomly chosen slot contains a successful single transmission with probability  $(1 - P_i)P_s$ .
- Capture: When two or more stations transmit and the packet of one station is captured successfully from the collision. This type of slot is a subset of slots containing collisions, which are a subset of busy slots. Thus, a randomly chosen slot contains a collision with a capture with probability  $(1 - P_i)(1 - P_s)P_{cap}$ .
- Failure: When two or more stations transmit and no packet is captured. Given that this state is a subset of slots containing collisions, the probability that a randomly chosen slot contains a collision and no packet is captured is given by  $(1 - P_i)(1 - P_s)(1 - P_{cap})$ .

#### 4. Analytical Model and Performance Evaluation

Since each station is allowed to contend for channel access only during its designated RAW slot, we start by modelling and evaluating the contention within one RAW slot. We consider a tagged RAW slot of duration  $T_S$  allocated for  $N_S$  stations. Note that only the  $N_S$  stations can compete for channel access during the period  $T_S$ .

The handover between two consecutive RAW slots is another factor to be considered. There are two options to deal with the transmission of a packet at the end of the RAW period according to the standard [4]. In the first case, the transmission of the last packet in a given RAW is not allowed to overrun the slot boundary. In the second case, the transmission of the last packet in a given RAW slot may cross the slot boundary. In this latter case, the stations in a RAW slot will not start contending for channel access until the ongoing transmissions from the previous RAW slot are completed.

Enabling RAW slot boundary-crossing will result in more energy loss for stations in the following RAW slot. That is because the stations will awake at the beginning of their allocated RAW slot and will not be able to contend for channel access until the last transmission from the preceding RAW slot is complete. Additionally, boundary-crossing in the final RAW slot will lengthen the overall time of the RAW, resulting in energy waste for stations competing outside the RAW. Thus, for these reasons and to guard fair resources allocation for all assigned stations in the RAW, we consider the RAW slot boundary-crossing to be disabled. Hence, stations are not allowed to cross the boundary of their allocated RAW slot with transmissions of their packets. To ensure this condition, a holding time  $T_H$  is defined at the end of the RAW slot, where stations are not allowed to initiate transmissions.

Hereafter, as depicted in Figure 4, the RAW slot period  $T_S$  is decomposed into a free access period  $T_F$  during which stations contend for channel access, and a holding period  $T_H$  during which stations are not to initiate a packet transmission. The holding period can only host ongoing transmissions initiated before the free access period boundary.

The remaining of this section is structured as follows. Section 4.1 introduces the stochastic model for the contention within the RAW slot period. Then, Sections 4.2 and 4.3 derive the performance metrics in a single RAW slot and several RAW slots, respectively.

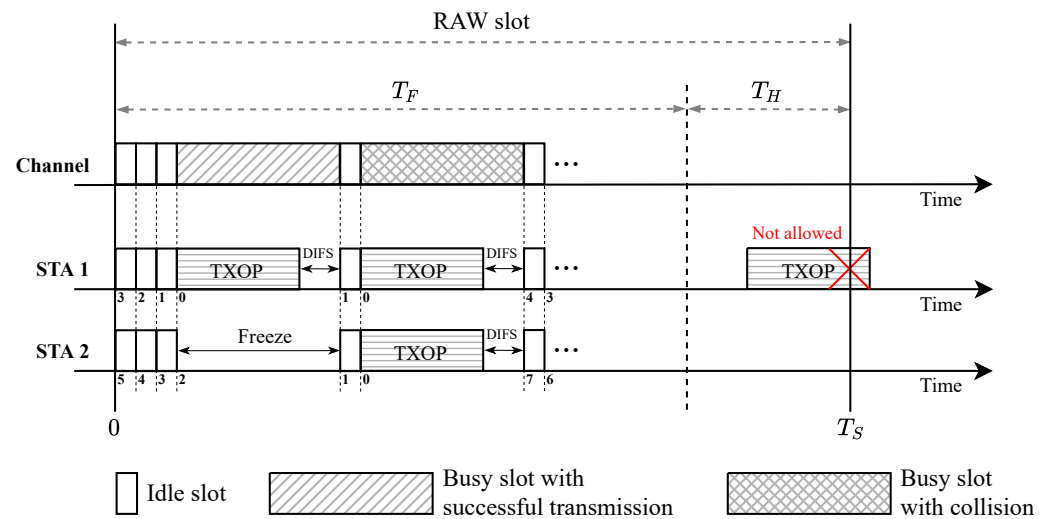


**Figure 4.** Structure of RAW slot.

#### 4.1. Stochastic Model

We aim to evaluate the RAW slot in terms of normalized throughput which represents the portion of the RAW slot period that is used to deliver data frames successfully to the AP, whether through single transmissions or captured packets. We consider a tagged RAW slot with duration  $T_S$  allocated for  $N_S$  stations. To derive the RAW slot throughput, we first need to determine the slots that contain successful delivery of data frames. That includes both successful single transmissions and successful delivery of captured packets.

In our previous work [7], we developed a renewal theory based model to derive the slots used for transmissions during the RAW slot period. We extend that model in this paper with the additional assumptions of channel fading and capture effect. Additionally, we enhance the accuracy in this new model by distinguishing the time exploited by transmissions during the holding period. Once the RAW slot interval begins, the assigned stations start to contend for channel access up to the instant  $T_F$ , which defines the free access period within the RAW slot. At time  $T_F$ , all stations suspend their backoff timers, and only ongoing transmissions are allowed during the holding period  $T_H$ . Hereafter, we observe the channel timeline during the RAW slot period in a binary state, where a randomly chosen slot can be idle or busy.

The stochastic model we propose is illustrated in Figure 5. We aim to evaluate the throughput within the RAW slot, which represents the channel usage ratio during its duration. To do so, we propose to deploy a renewal theory approach to model the contention of stations during the RAW slot period by constructing a counting process to keep track of occurred transmissions up to the end of the RAW slot interval  $T_S$ .

For every  $i \in \mathbb{N}$ , denote the type of the  $(i + 1)$ th slot by the random variable  $Z_i$ , where the events  $\{Z_i = 1\}$  and  $\{Z_i = 0\}$  represents a busy and idle slot, respectively. A randomly chosen slot is idle with probability  $P_i$  and busy with probability  $(1 - P_i)$ . Thus, we have  $Pr\{Z_i = 1\} = 1 - P_i$ , and  $Pr\{Z_i = 0\} = P_i$ . Therefore, the sequence  $\{Z_i\}_{i \geq 0}$  forms a Bernoulli process, with success and failure of the  $i$ th trial given by the events  $\{Z_i = 1\}$  and  $\{Z_i = 0\}$ , respectively.

Let  $i$  be the counter of slots during the RAW slot timeline, and  $\{t_i\}_{i \geq 0}$  be an increasing sequence representing the beginning instants of slots with  $t_0 = 0$ . Let  $\beta = T_{TXOP} + DIFS$  be the length of a busy slot and  $\sigma$  be the duration of an idle slot. Then, we can define the duration of the  $i^{\text{th}}$  slot as follows:

$$t_i - t_{i-1} = \begin{cases} \beta, & \text{if } \{Z_{i-1} = 1\}, \\ \sigma, & \text{if } \{Z_{i-1} = 0\}. \end{cases} \quad (23)$$





Therefore,  $\{A_k\}_{k \geq 0}$  is a well-defined renewal process and  $\{N_t\}_{t \geq 0}$  is its associated counting process defined as follows:

$$N_t = \arg \max_{k \in \mathbb{N}} \{A_k \leq t\} \quad (27)$$

We now proceed to derive the expected number of busy slots  $E[N_{T_S}]$  within the RAW slot period  $T_S$ . The stations stop counting down their backoff counters at the end of the free access period  $T_F$ , and the holding period  $T_H$  is reserved to only the ongoing transmissions initiated before the boundary of  $T_F$ . Hence, we define the maximum number of transmissions that can occur during the RAW slot period as follows:

$$\Gamma_b = \left\lfloor \frac{T_F}{\beta} \right\rfloor + \mathbb{1}_{\{T_F > \lfloor \frac{T_F}{\beta} \rfloor \cdot \beta + \sigma\}} \quad (28)$$

**Proposition 1.** The expected number of busy slots within a RAW slot of duration  $T_S$  allocated for  $N_S$  stations is given by:

$$E[N_{T_S}] = \sum_{k=1}^{\Gamma_b} \sum_{j=0}^{\lfloor \frac{T_F - (k-1) \cdot \beta}{\sigma} \rfloor} \binom{j+k-1}{j} (1-P_i)^k P_i^j. \quad (29)$$

**Proof.** We have by definition  $N_{T_S} = \arg \max_{k \in \mathbb{N}} \{A_k \leq T_F\}$ . Since  $\{A_k\}_{k \geq 0}$  is an increasing process, we can define  $N_{T_S}$  as the cardinal of the set  $\{k \geq 1 : A_k \leq T_F\}$ . Thus,

$$\begin{aligned} E[N_{T_S}] &= E \left[ \arg \max_{k \in \mathbb{N}} \{A_k \leq T_F\} \right] \\ &= E[\#\{k \geq 1 : A_k \leq T_F\}] \\ &= E \left[ \sum_{k=1}^{\infty} \mathbb{1}_{\{A_k \leq T_F\}} \right] \\ &= \sum_{k=1}^{\infty} Pr\{A_k \leq T_F\} \end{aligned}$$

Since the number of transmissions within the RAW slot is limited by  $\Gamma_b$ ,  $Pr\{A_k \leq T_F\} = 0$  for  $k > \Gamma_b$ . Henceforth,

$$\begin{aligned} E[N_{T_S}] &= \sum_{k=1}^{\Gamma_b} Pr\{A_k \leq T_F\} \\ &= \sum_{k=1}^{\Gamma_b} Pr \left\{ \sum_{i=1}^k Y_i \leq T_F \right\} \\ &= \sum_{k=1}^{\Gamma_b} Pr \left\{ (k-1) \cdot \beta + \sigma \sum_{i=1}^k X_i \leq T_F \right\} \\ &= \sum_{k=1}^{\Gamma_b} Pr \left\{ \sum_{i=1}^k X_i \leq \frac{T_F - (k-1) \cdot \beta}{\sigma} \right\} \\ &= \sum_{k=1}^{\Gamma_b} \sum_{j=0}^{\lfloor \frac{T_F - (k-1) \cdot \beta}{\sigma} \rfloor} Pr \left\{ \sum_{i=1}^k X_i = j \right\} \end{aligned}$$

$\sum_{i=1}^k X_i$  forms a sum of  $k$  IID random variables following a geometric distribution with parameter  $(1 - P_i)$ . Hence,  $\sum_{i=1}^k X_i$  is a random variable that follows the negative binomial distribution with parameters  $k$  and  $(1 - P_i)$ . Thus, we have

$$E[N_{T_S}] = \sum_{k=1}^{\Gamma_b} \left[ \frac{T_F - (k-1) \cdot \beta}{\sigma} \right] \binom{j+k-1}{j} (1-P_i)^k P_i^j.$$

□

**Proposition 2.** The expected number of idle slots within a RAW slot of duration  $T_S$  allocated for  $N_S$  stations is given by:

$$E[I_{T_S}] = \frac{P_i}{1-P_i} \cdot E[N_{T_S}]. \quad (30)$$

**Proof.** Let  $I_{T_S}$  be a random variable representing the number of idle slots within the RAW slot period  $T_S$ . Note that idle slots occur only during the free access period  $T_F$  as all stations terminate their backoff counters at the boundary of  $T_F$ .

Thus,  $I_{T_S}$  represents the aggregated number of idle slots preceding all transmissions occurred during the RAW slot. Since we have  $N_{T_S}$  busy slots within the RAW slot and each busy slot  $k$  is preceded by  $X_k$  idle slots, we have  $I_{T_S} = \sum_{k=1}^{N_{T_S}} X_k$ .

We have  $\{X_k; k \geq 1\}$  is a sequence of IID random variables with same mean  $\bar{X} = E[X_k], \forall k \geq 1$ . Additionally,  $E[N_{T_S}] < \infty$  as proved in Proposition 1.

Therefore, according to Wald's equality [23], we have

$$E[I_{T_S}] = E\left[\sum_{k=1}^{N_{T_S}} X_k\right] = \bar{X} \cdot E[N_{T_S}]. \quad (31)$$

In addition, for every  $1 \leq k \leq N_{T_S}$ ,  $X_k$  follows a geometric distribution on  $\mathbb{N}$  with rate  $1 - P_i$ .

Thus,

$$\bar{X} = \frac{P_i}{1-P_i}. \quad (32)$$

By substituting (32) in (31), we obtain the result. □

After deriving the expected number of idle and busy slots that occupy the free access period of the RAW slot, we can now study the channel usage during the holding period. Thus, we define the holding period usage ratio, representing the portion of time from the holding period that is exploited by transmissions, as follows:

$$U_h = \frac{E[I_{T_S}] \cdot \sigma + E[N_{T_S}] \cdot \beta - T_F}{T_H}. \quad (33)$$

#### 4.2. Evaluating a Single RAW Slot

Since busy slots represent three types of slots, as mentioned previously, we can derive from  $E[N_{T_S}]$  three average numbers of slots containing successful single transmissions, collisions with capture, and collisions without capture.

As stated previously, a randomly chosen slot accommodates a successful single transmission (i.e., is in the state "Success") with probability  $(1 - P_i)P_s$ . Therefore, knowing that a random slot is busy with probability  $(1 - P_i)$ , we define the expected number of slots containing successful single transmissions during the RAW slot period as follows:

$$A_{T_S}^s = E[N_{T_S}] \cdot P_s. \quad (34)$$

A randomly chosen slot contains a collision with capture when one of the interfering packets is successfully captured and delivered to the AP. Given that such an event happens

with probability  $(1 - P_i)(1 - P_s)P_{cap}$  and that it is a subset event of non-idle slots, we define the average number of slots in the state “Capture” within the RAW slot as follows:

$$A_{T_S}^{cap} = E[N_{T_S}] \cdot (1 - P_s) \cdot P_{cap}. \quad (35)$$

A randomly chosen slot contains a collision with no capture when none of the interfering packets is captured from the collision. That is, all transmitted packets faced a failed delivery in the considered slot. Since such event is a subset of busy slots and that a random slot is in this state with probability  $(1 - P_i)(1 - P_s)(1 - P_{cap})$ , we have the average number of slots in the state “Failure” within the RAW slot given by:

$$A_{T_S}^f = E[N_{T_S}] \cdot (1 - P_s) \cdot (1 - P_{cap}). \quad (36)$$

A data frame delivery can be successful when only one station is transmitting, or two or more stations are transmitting simultaneously and the AP successfully captures one packet following the collision. We define the RAW slot throughput as the ratio of time used to transmit data frames during the period  $T_S$  successfully. That is the time occupied by the successful delivery of data frames during successful single transmissions and during the successful delivery of captured packets from collisions. Therefore, the RAW slot throughput is expressed as follows:

$$Th_S = \frac{(A_{T_S}^s + A_{T_S}^{cap}) \cdot T_{DATA}}{T_S}. \quad (37)$$

To determine the gain from the capture feature in the network, we need to compare the network performance with the case of the no-capture channel. There are several differences between a channel with capture and a no-capture channel. Starting from the EDCA mechanism for channel access, in which a collided packet can still be captured in the first scenario, and hence the source station resets its CW to  $CW_0$ , whereas there is no such behavior in the case of a no-capture channel.

Henceforth, in the case of a no-capture channel,  $p_{cap}^p = 0$  and  $p = p_{col}^p$ . Therefore,  $\tau$  and  $p$  can be obtained by solving numerically the non-linear system defined by (9) and (10).

As for the channel slots, a randomly chosen slot has three states: idle, success, and collision, where the states “Idle” and “Success” are the same as defined in the previous scenario. Additionally, a chosen random slot can be in a state of collision when it hosts more than one transmission, which happens with probability  $(1 - P_s)(1 - P_{cap})$ .

Hereafter, the RAW slot throughput in the case of a no-capture channel is given by:

$$Th_S^{NC} = \frac{A_{T_S}^s \cdot T_{DATA}}{T_S}. \quad (38)$$

#### 4.3. Evaluating Several RAW Slots

Consider a RAW uniformly divided into  $K$  RAW slots, each of duration  $T_S = T_R/K$ . According to the stations’ assignment defined in (1), the RAW structure will end up with  $K_1 = K - (N_R \bmod K)$  RAW slots, each one allocated to  $N_S^1 = \lfloor N_R/K \rfloor$  and  $K_2 = K - K_1$  RAW slots, each allocated to  $N_S^2 = N_S^1 + 1$ . Note that if the total number of stations in the RAW  $N_R$  is divisible by the number of RAW slots  $K$ , we will have a uniform allocation of both RAW slots’ duration and assigned stations. Thus, the RAW will consist of  $K$  similar RAW slots of duration  $T_S = T_R/K$  with  $N_S = N_R/K$  assigned stations.

The RAW throughput is defined by the portion of the time used to deliver data frames during the RAW period  $T_R$  successfully. Hence, the normalized throughput of a RAW with  $K$  RAW slots is expressed as follows:

$$Th_R(K) = \frac{\left( K_1 \left( A_{T_S^1}^s + A_{T_S^1}^{cap} \right) + K_2 \left( A_{T_S^2}^s + A_{T_S^2}^{cap} \right) \right) \cdot T_{DATA}}{T_R}. \quad (39)$$

The normalized throughput of a RAW consisting of  $K$  RAW slots in the case of a no-capture channel is given by:

$$Th_R^{NC}(K) = \frac{(K_1 \cdot A_{T_S^1}^s + K_2 \cdot A_{T_S^2}^s) \cdot T_{DATA}}{T_R}. \quad (40)$$

To derive the added value of the capture feature within the RAW, we compare the RAW throughput for a channel with capture to the no-capture channel. Thus, we define the RAW capture ratio for a RAW consisting of  $K$  RAW slots as the portion of the RAW throughput gained through the capture effect, and it is given by:

$$G_{cap}(K) = \frac{Th_R(K) - Th_R^{NC}(K)}{Th_R(K)}, \quad (41)$$

where  $Th_R(K)$  is the RAW throughput in the case of a channel with capture, defined in (39). The definition in (41) means that  $G_{cap}(K)$  percent of the RAW throughput  $Th_R(K)$  is gained thanks to the capture effect, where packets are successfully delivered after being captured from collisions.

## 5. Results and Discussion

This section evaluates and analyzes our findings through numerical results and simulations using MATLAB software. It also presents a validation for our mathematical framework and the obtained analytical results through extensive simulations derived via a discrete-event simulator we developed with MATLAB. The simulator mimics the channel access using the EDCA mechanism, considering the random distribution of stations around the AP, the power attenuation of received packets under a Rayleigh fading channel, and the capture of a packet in case of collision if its signal-to-interference ratio exceeds the capture threshold  $z$ . A single simulation of a RAW slot yields the contention results from its beginning until the end of its duration. The final results represent the average of 10,000 simulations. We observe in the figures below a close match of the results obtained from our model and the simulations, which validates the accuracy of our mathematical framework.

We shall first study the performance of one RAW slot for different parameters: its duration  $T_S$ , the number of designated stations  $N_S$ , and the capture threshold  $z$ . We then examine a RAW consisting of several RAW slots by studying the impact of the grouping on the overall RAW performance under the presence of the capture effect. We additionally investigate the RAW capture ratio under different RAW configurations. We consider sensor stations of category video or VOIP, allowing one retransmission attempt of a collided packet according to the standard [4]. Besides the parameters we put in the study, the remaining parameters considered in both analytical framework and simulations are presented in Table 1.

**Table 1.** Parameters

Parameter	Value
Data rate	1.95 Mbps
MacHeader	272 bits
$T_{ACK}$	1000 $\mu$ s
$T_{PLCP}$	80 $\mu$ s
$\sigma$	52 $\mu$ s
SIFS	160 $\mu$ s
DIFS	264 $\mu$ s
$CW_{min}$	8
$CW_{max}$	16
$m$	1
Payload	160 bytes
$\rho$	100 m



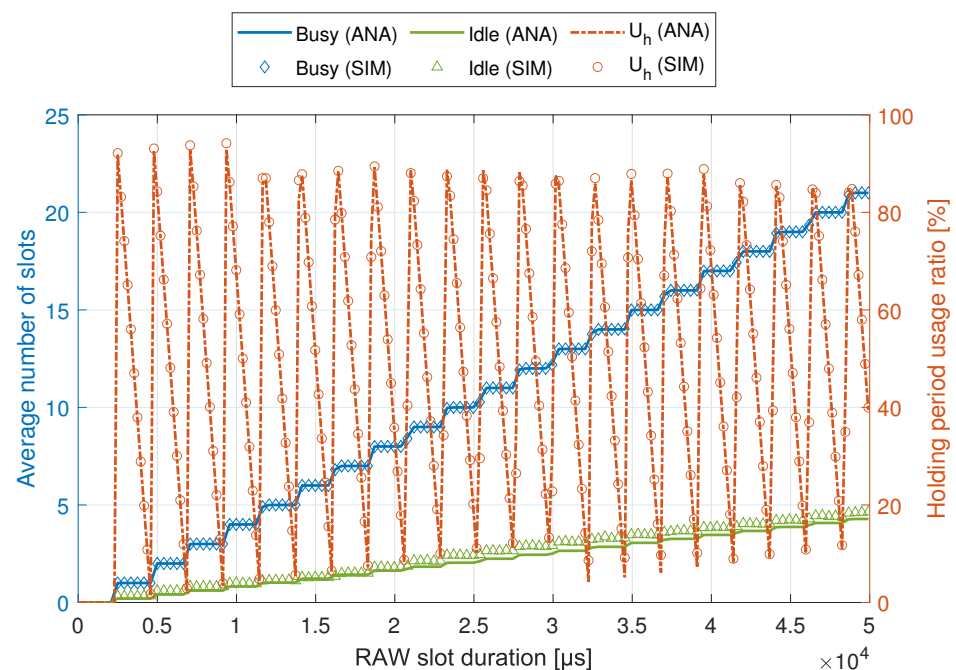
### 5.1. RAW Slot

#### 5.1.1. RAW Slot Period

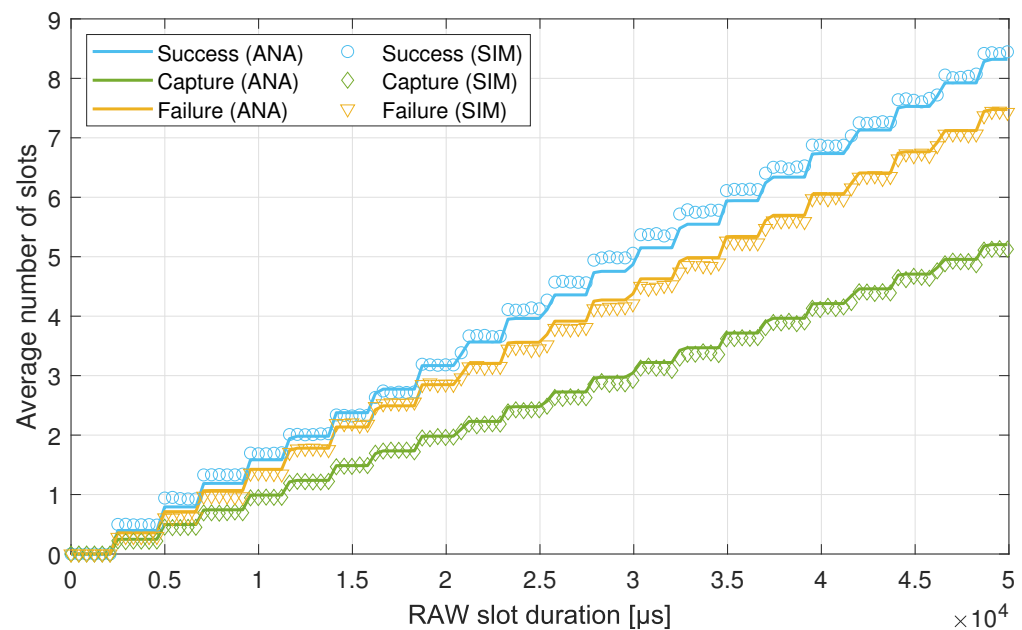
We evaluate in this section the RAW slot throughput as a function of its duration  $T_S$ , which represents the portion of time used for the successful transmission of data frames. We consider a RAW slot allocated to 10 stations, distributed uniformly within the radius  $\rho = 100$  m, and a channel with capture threshold  $z = 8$  dB.

Figure 6 depicts the expected number of busy and idle slots in terms of the duration of the RAW slot period. The figure also depicts the holding period usage ratio  $U_h$ , representing the portion of  $T_H$  exploited by transmissions. These three results start with the value zero and yield positive values after a given value of  $T_S$ . That corresponds to when  $T_S$  is long enough to host at least one transmission. The average number of busy slots  $E[N_{T_S}]$  is almost a step function that increases by one unit whenever  $T_S$  is long enough to host an additional complete transmission. Similar behavior is shown by the average number of idle slots  $E[I_{T_S}]$  since idle slots precede each busy slot.  $U_h$  has a fluctuating behavior as  $T_S$  increases. When the additional time in the RAW slot interval is not enough to host additional transmissions,  $E[N_{T_S}]$  remains constant, and the holding period becomes unused. That causes a fast drop in the value of  $U_h$ . When RAW slot duration  $T_S$  increases enough to allow additional transmissions,  $E[N_{T_S}]$  and  $E[I_{T_S}]$  increase while  $U_h$  jumps to the maximum possible usage ratio. We observe that the variation interval of  $U_h$  is decreasing as  $T_S$  increases. That is because the holding period  $T_H$  becomes less significant within the RAW slot interval and hence less affecting in cases used or wasted. Eventually, as  $T_S$  tends to infinity, the usage of the holding period becomes completely unaffected, and the value of  $U_h$  converges to 50%.

Figure 7 represents the average number of slots in each state of success, capture and failure. Since all the three states are a subset of the busy slot state, we observe that the average number of slots in each state has the same behavior as  $E[N_{T_S}]$  presented in Figure 6. That is explained by the same aforementioned phenomena of the RAW slot period, which allows additional transmissions only when long enough. Note that in the presented scenario, the average number of slots with a successful single transmission  $A_{T_S}^s$  is larger than the other two types due to the low contention of the considered ten stations.



**Figure 6.** Average number of busy and idle slots, and the holding period usage ratio within the RAW slot interval, with channel capture threshold  $z = 8$  dB.



**Figure 7.** Average number of slots with successful single transmission, captured packet, and failure, within the RAW slot interval, with channel capture threshold  $z = 8$  dB.

Figure 8 presents the RAW slot throughput in terms of its allocated period  $T_S$ . We consider two channel scenarios: a no-capture channel and a channel with capture for different capture threshold values  $z$ : 2 dB, 4 dB, 8 dB, and 16 dB. The RAW slot throughput represents the portion of time used to successfully transmit data frames to the AP during the RAW slot period  $T_S$ . In both channel scenarios, the RAW slot throughput has a fluctuating behavior due to the usage of the holding period when  $T_S$  increases as depicted in Figure 6. When the RAW slot duration  $T_S$  increases and the extended period is not enough to host another transmission, the additional time in  $T_S$  is wasted and the holding period usage ratio  $U_h$  decreases, which results in a drop in the RAW slot throughput. On the other hand, as long as  $T_S$  can allow an additional transmission, the RAW slot throughput jumps to a higher value. When  $T_S$  is long enough, the presence or absence of one transmission does not affect the total transmissions in the RAW slot period, and hence, the fluctuating behavior slightly disappears. Eventually, the RAW slot throughput converges to the case of an infinite RAW slot. Regarding the capture feature, we observe that a channel with capture yields higher throughput for the RAW due to the supplementary delivered packets captured from collisions. However, the capture threshold has an inverse impact on the throughput. A lower capture threshold means that the AP can capture a packet from a collision even if its received power shortly exceeds the joint power of interfering packets. This effect results in more captured packets from collisions and hence higher throughput. Nevertheless, increasing the capture threshold lowers the possibility of capturing packets, which reduces the RAW slot throughput. Ultimately, when the capture threshold tends to infinity, the capture of packets becomes unfeasible, and hence the RAW slot throughput converges to the throughput provided by a channel without capture.

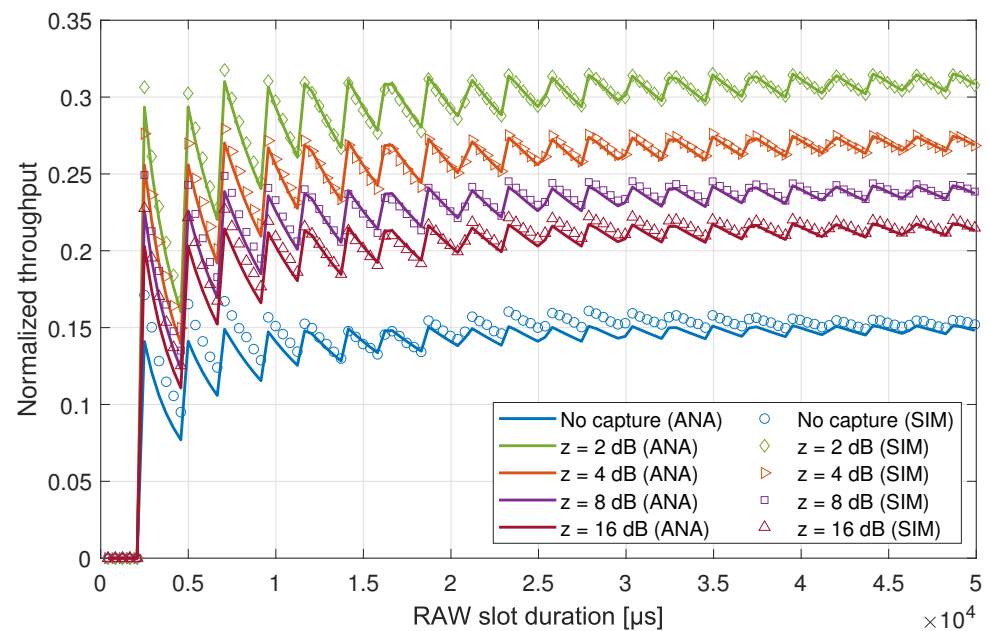


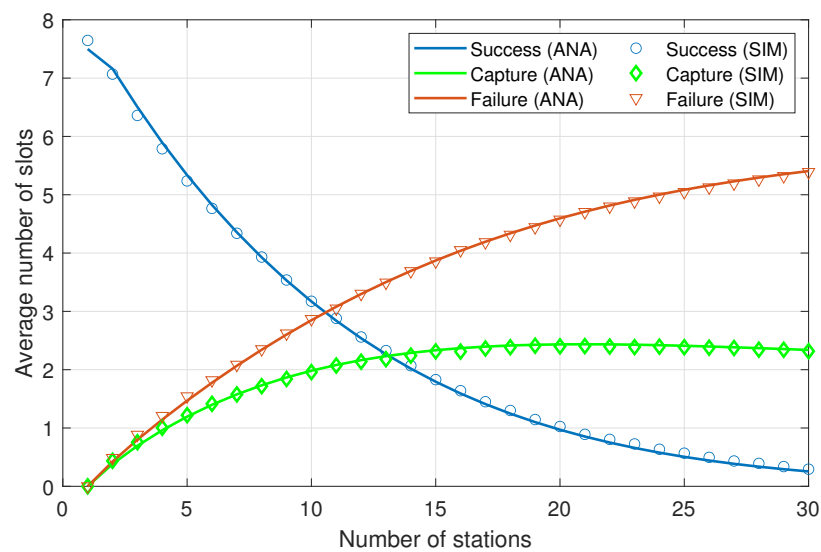
**Figure 8.** Impact of the capture threshold on the RAW slot throughput.

Our developed analytical framework is based on the assumption that every station transmits its packet in a randomly chosen slot with the same probability  $\tau$ , defined in (9). The latter depends on the attempts and idle slots experienced by the station. The slight differences between the analytical and simulation results depicted in Figures 6–8 are due to the channel access probabilities that depend on  $\tau$  and the number of contending stations. The analytical throughput in Figure 8 yields slightly lower values than the simulation, especially for a very short RAW slot. That is because the model assumes that every station goes through all possible transmission attempts and backoffs, and hence more potential collisions. Whereas in the simulation, the contention is just starting and the backoff counters of most of the stations are still in their first contention window. However, the analytical throughput always keeps the same trends as the simulation, which preserves accuracy for deriving optimal configuration that maximizes the throughput.

### 5.1.2. Contending Stations

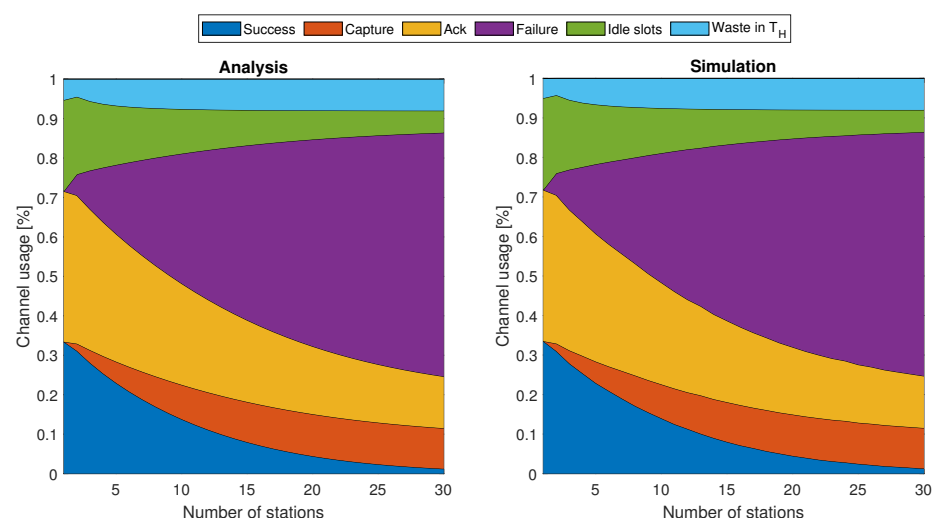
We consider a group of stations distributed uniformly around the AP within the radius  $\rho = 100$  m. We evaluate the throughput of a RAW slot with length  $T_S = 20$  ms in terms of the designated stations.

Figure 9 presents the average number of the three types of busy slots during the RAW slot period regarding the number of contending stations. When more stations are assigned to the RAW slot, the contention increases and yields more collisions. That lowers the number of slots with a successful single transmission and raises slots containing a capture and slots with failure. Furthermore, the average number of slots  $A_{T_S}^{cap}$  containing a collision with capture has a downward concave shape behavior. Given that more stations bring on more collisions, the AP captures more packets from these collisions, which increment the value of  $A_{T_S}^{cap}$ . Eventually, a higher number of stations will be involved in collisions, which lowers the chances of capturing a packet due to the higher joint received power of interfering packets. That results in limiting the increment rate of  $A_{T_S}^{cap}$  and ultimately diminishes its value when a large number of stations are assigned to the RAW slot.



**Figure 9.** Average number of slots with successful single transmission, captured packet, and failure, within a RAW slot interval of length  $T_S = 20$  ms and channel capture threshold  $z = 8$  dB.

Figure 10 shows the channel usage ratio during the RAW slot period of length  $T_S = 20$  ms with capture enabled at threshold  $z = 8$  dB. When more stations participate in the RAW slot, the contention arises, and the channel becomes more occupied by transmissions, diminishing the idle time. Moreover, the time consumed by collisions (slots with capture and failure) increases, whereas the time used for successful single transmissions rapidly degrades due to the immense contention generated by more stations in such a short period of the RAW slot. However, the capture feature takes advantage of the rise of collisions, and more packets are captured when the RAW slot becomes denser. As observed in the figure, the capture feature in the channel allows to successfully deliver packets even when typical single transmissions are not possible (e.g., when  $N_S = 30$ ). The time used to transmit ACK frames follows the trend of successful transmissions that occurred during both single transmissions and captured packets. The figure also shows a slightly better usage of the holding period for fewer stations. That is, fewer stations can initiate transmissions occupying a larger part of the holding period. Note that such a result is also related to other factors such as the RAW slot duration and payload size. The usage ratio of the holding period is mainly affected by the RAW slot duration, as discussed in Figure 6.



**Figure 10.** Channel usage ratio by different events occupying the RAW slot interval with capture threshold  $z = 8$  dB, in terms of contending stations.

Hereafter, we examine in Figure 11 the impact of the capture threshold  $z$ . We first consider a RAW slot with a fixed length  $T_S = 20$  ms. Then, we explore its throughput in terms of the designated stations for a no-capture channel and a channel with capture for different capture thresholds:  $z = 2$  dB, 4 dB, 8 dB, 16 dB. A channel with a smaller capture threshold provides higher throughput during the RAW slot period. Conversely, a higher capture threshold value lessens the captured packets and henceforth degrades the RAW slot throughput. Ultimately, when the capture threshold  $z$  rises, the RAW slot throughput converges to the result provided by a normal channel without capture.

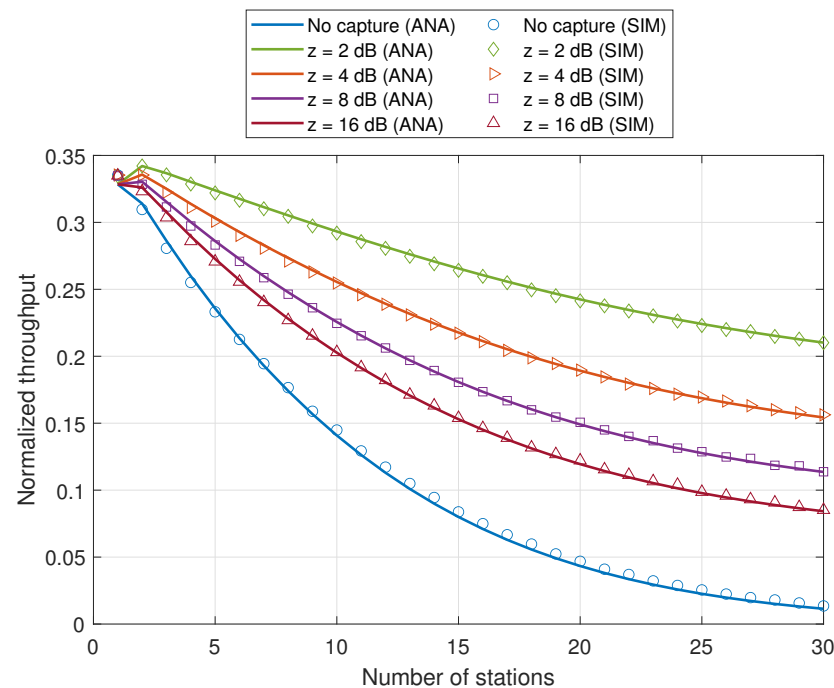


Figure 11. Impact of the capture threshold on the RAW slot throughput.

### 5.1.3. Capture Threshold

We consider a RAW slot of length  $T_S = 20$  ms allocated for  $N = 10$  stations, and we investigate the impact of the capture threshold  $z$  on the RAW slot throughput.

Figure 12 depicts the average number of each of the three states of busy slots during the RAW slot period. The average number of slots with a successful single transmission shows a slightly increasing variation for short values of the capture threshold  $z$ , which is explained by the higher values achieved by  $A_{T_S}^{cap}$  at the same period of  $z$ . When a packet is captured, its source station resets its CW to  $CW_0$ , which increases the station's chances of delivering another packet without colliding. As the capture threshold  $z$  increases, it becomes unlikely for a received power of one packet to exceed the joint interfering powers by the threshold  $z$ . That translates into a decrease in the average number of slots containing collision with capture  $A_{T_S}^{cap}$  and an increase in the average number of slots containing failure (collision with no capture)  $A_{T_S}^f$ .



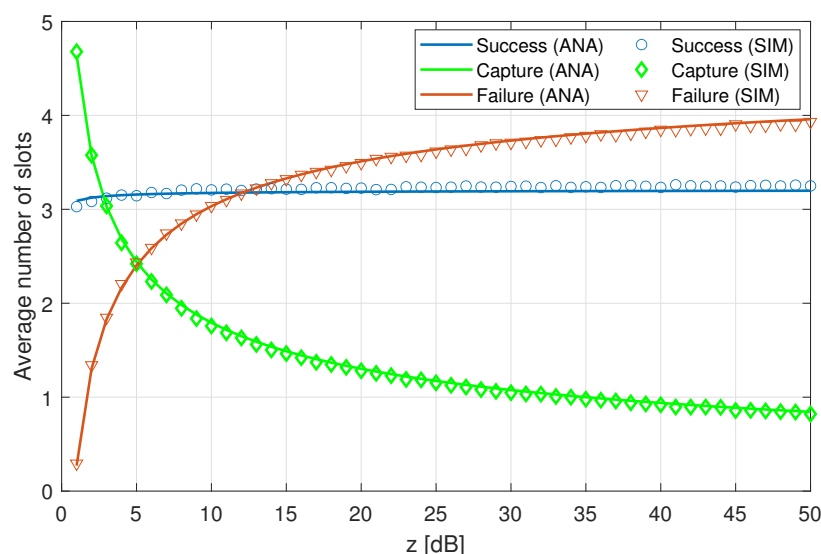


**Figure 12.** Average number of slots with with successful single transmission, captured packet, and failure, in terms of the capture threshold, within a RAW slot of duration  $T_S = 20$  ms and  $N = 10$  assigned stations.

Hereafter, we explore the impact of both the capture threshold and the number of assigned stations in the RAW slot. Figure 13 depicts the normalized throughput within a RAW slot of duration  $T_S = 25$  ms in terms of the capture threshold for different sets of stations. As long as  $z$  gets a higher value, it becomes less likely for the AP to capture packets from collisions, as seen in Figure 12. For that reason, increasing the value of the capture threshold lowers the ability to capture packets from collisions and degrades the RAW slot throughput. As a result, it ultimately eliminates the capture feature and converges to the scenario of a no-capture channel. From the perspective of stations assigned to the RAW slot, we observe a higher capture gain for a denser RAW slot. That is due to high contention, which presents more collisions and hence more captured packets. Hereafter, we see that ten stations operating within a channel with a capture threshold  $z \leq 6$  dB yield higher throughput than five stations operating within a no-capture channel. Similarly, we observe that 20 stations operating within a channel with a capture threshold  $z \leq 2$  dB and  $z \leq 9$  dB provide better throughput than five stations and ten stations, respectively, operating within a no-capture channel. Such results are significant to consider in developing efficient scheduling algorithms for configuring the RAW mechanism.

The observed difference between the analytical and simulation results for 10 and 20 stations is due to the same reason explained in the previous subsection. The evaluation of a short RAW slot of duration  $T_S = 25$  ms when allocated to a higher number of stations predicts more collisions. Whereas, in the simulation, the backoff counters of most of the stations are still on the first contention window  $W_0$  and it is less likely for collisions to occur. However, we observe a higher accuracy of the throughput for five stations, which is a more practical scenario for such a short RAW slot. Additionally, we can see a higher accuracy of the throughput for 10 and 20 stations in the case of a channel with capture enabled, especially for a small threshold that allows more captured packets and eliminates the misprediction of higher collisions in the no-capture channel case.

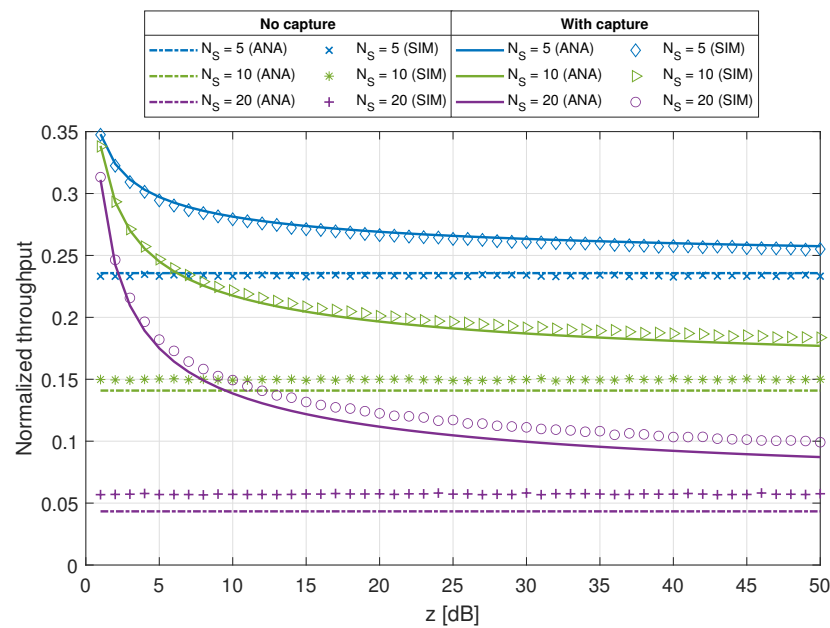


**Figure 13.** Impact of the capture threshold and the number of stations assigned to the RAW slot.

## 5.2. RAW Performance

The IEEE 802.11ah standard introduced the grouping within RAW to reduce collisions among allocated stations to the RAW. However, the standard does not specify the algorithm to perform such grouping. Henceforth, this section examines the impact of grouping the nodes as evenly as possible across the available RAW slots. As shown in the previous section, short RAW slots yield a fluctuating throughput behavior. From such behavior, we can deduce that it is not obvious to make an optimal choice about the number of RAW slots that maximizes the RAW gain.

Figure 14 shows the normalized throughput for a  $T_R = 500$  ms RAW in terms of the number of RAW slots in a RAW for four different number of stations,  $N_R = 64, 140, 300, 600$ . As seen in the figure, subdividing the RAW into more RAW slots increases the normalized throughput up to a certain point from which the throughput presents light fluctuations around a saturation point. This behavior is explained by the fact that by subdividing the RAW into more groups, the RAW slot duration  $T_S$  becomes shorter, and as a result, the  $T_H/T_S$  ratio increases. Since  $T_H$  may be exploited or not, the RAW throughput keeps decreasing and increasing as the number of groups in the RAW increases. Note that such behavior does not appear for a small number of groups because the RAW slots in this range are long enough not to be affected by the use or non-use of the holding period. Furthermore, the overall RAW throughput achieves a maximum value at a given number of RAW slots as depicted in the figure, where  $K_{op}^N$  is the optimal number of slots when  $N$  stations are assigned to the RAW. In the case of RAWs consisting of  $N_R = 140, 300, 600$ , a higher number of slots than the use for  $N_R = 64$  is required before reaching the maximum achievable throughput. As depicted in the figure, an increase in the number of slots beyond the optimal number of slots may cause a drop of up to 5% on the maximum achievable throughput for a network consisting of  $N_R = 140$ . We also observe that a RAW with fewer assigned stations has a sharper increase in normalized throughput when the RAW is subdivided into more RAW slots. That is due to lighter contention in each RAW slot after allocating more RAW slots in the RAW period. However, a dense RAW is slightly affected by the grouping due to the high contention that is still present in each RAW slot.

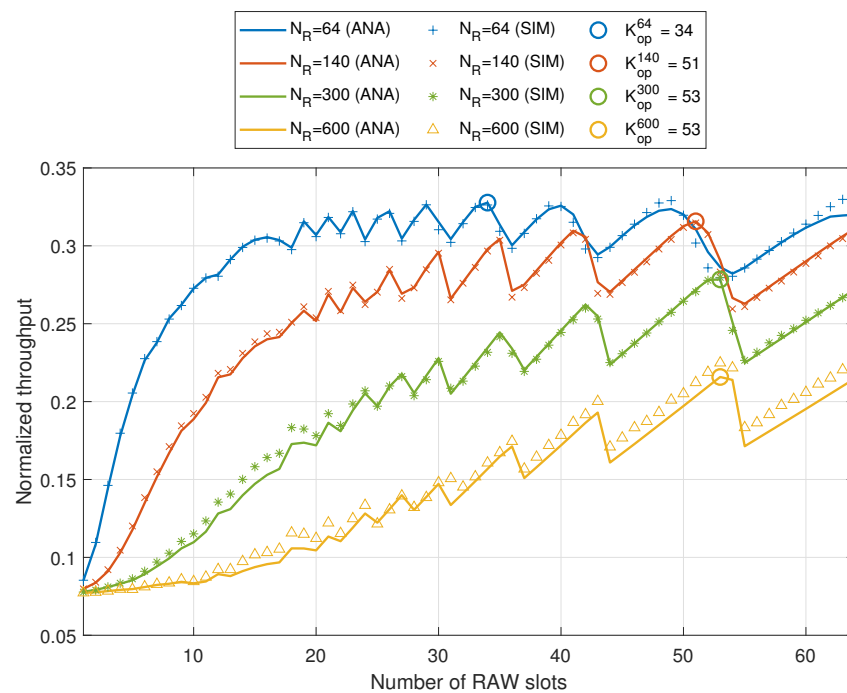


**Figure 14.** RAW throughput in terms of allocated RAW slots for different sets of assigned stations.

Figure 15 depicts the RAW capture ratio, representing the ratio of throughput gained from captured packets during the RAW period  $T_R = 500$  ms. We observe that when the RAW is composed of one RAW slot, i.e., all stations are contending for channel access simultaneously, 100% of the RAW throughput is derived from the capture of packets from collisions. That means there will be no successful transmissions within the RAW duration in such conditions with a no-capture channel. Allocating more RAW slots within the RAW leads to fewer stations in each RAW slot, decreasing collisions and allowing successful single transmissions. Thus, the percentage of captured packets among the total delivered ones becomes less, and hence the RAW capture ratio decreases. Eventually, the capture ratio becomes null when collisions are eliminated within the RAW, which coincides with the case of one station per RAW slot. Note that this case may not be possible if the number of stations is greater than 64 or when the length of each RAW slot is not sufficient to host at least one transmission. Furthermore, we observe a slight difference between the analytical results and simulations in both Figures 14 and 15 for the cases of 300 and 600 stations. That is due to the fact that each RAW slot in these cases contains a higher number of stations, and hence more disturbance to the throughput due to the prediction of more collisions as discussed in Figures 8 and 13.

Our results show that our modeling framework allows us to evaluate the performance of the IEEE 802.11ah RAW mechanism by taking into account key system parameters, namely, the number of nodes, number of groups, channel bit rate, and packet length. Furthermore, our methodology also includes modeling the wireless channel and the network layout, i.e., placement of the nodes with respect to the AP. Our resulting modeling framework contributes to the development of evaluation and optimization solutions of IEEE 802.11ah networks: an area of great interest to the research and development of dense wireless systems [30].

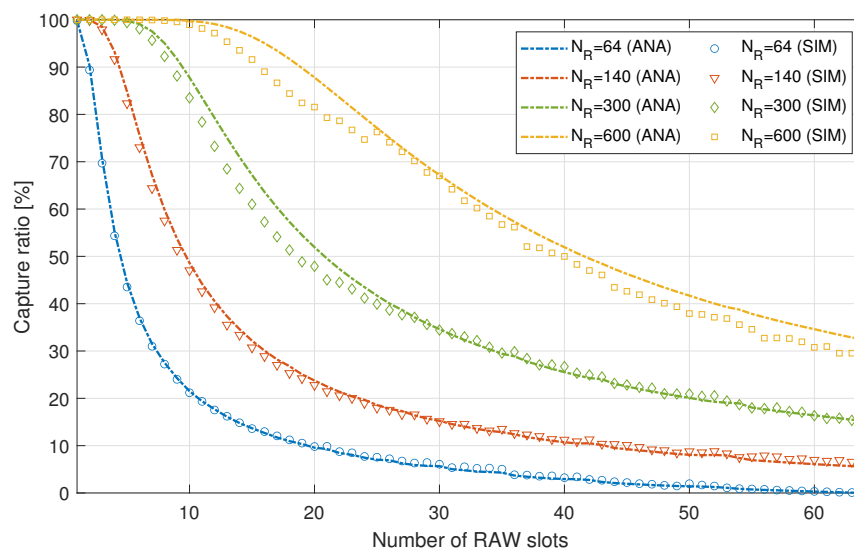


**Figure 15.** Capture gain in terms of allocated RAW slots for different sets of assigned stations to the RAW.

## 6. Conclusions

We presented in this paper an accurate mathematical framework to model and evaluate the performance of an IEEE 802.11ah-based network with the presence of capture effect in the channel. We first modeled the channel access under capture awareness, considering a Rayleigh-fading channel where the capture model considers the stations' distance from the AP and the power attenuation of the received packets. We further defined the different states of a randomly chosen slot within the RAW slot period. Since the RAW mechanism presents a time-limited contention for channel access, we then developed a counting process to track transmissions up to the end of the contention time interval. Hereafter, we evaluated the performance of a single RAW slot and a RAW comprising several RAW slots in terms of throughput, representing the ratio of time used to deliver data frames during the total contention period successfully. The derived analytical results are meticulously validated through extensive simulations obtained via a simulator we developed with the MATLAB software. We studied the impact of different parameters on the overall performance of the time-limited contention, including the contention time, the number of stations, and the capture threshold. We also examined the capture ratio within the RAW, representing the portion of RAW throughput gained via the capture effect in the channel. It is shown that a very dense RAW can only deliver data through captured packets. However, the capture ratio degrades when the RAW comprises a more significant number of RAW slots due to less contention in each RAW slot. Besides the RAW duration and the number of assigned stations, several other parameters affect the overall RAW throughput when considering a channel with capture as the capture model, the capture threshold, stations' locations, and the power attenuation. Henceforth, it is critical to consider all these parameters to derive efficient scheduling algorithms for the RAW mechanism. The proposed analytical model and associated results present an excellent basis to propose practical scheduling algorithms to configure the RAW mechanism under a fading channel and a capture effect at the receiver.

**Author Contributions:** Conceptualization, H.T. and L.O.-B.; methodology, H.T., J.J.C.-E., J.G., L.O.-B. and A.H.; software, H.T.; validation, H.T., J.J.C.-E., J.G., L.O.-B. and A.H.; formal analysis, H.T. and A.H.; investigation, H.T., J.J.C.-E., J.G., L.O.-B. and A.H.; writing—original draft preparation, H.T.; writing—review and editing, H.T., J.J.C.-E., J.G., L.O.-B. and A.H.; funding acquisition, L.O.-B. and A.H. All authors have read and agreed to the published version of the manuscript.

**Funding:** This work was supported by the Spanish Ministry of Science, Education and Universities, the European Regional Development Fund and the State Research Agency, Grant No. RTI2018-098156-B-C52. The first author was supported by the Erasmus+ program K107.

**Institutional Review Board Statement:** Not applicable.

**Informed Consent Statement:** Not applicable.

**Data Availability Statement:** Not applicable.

**Conflicts of Interest:** The authors declare no conflict of interest.

## References

- Kassab, W.; Darabkh, K.A. A–Z survey of Internet of Things: Architectures, protocols, applications, recent advances, future directions and recommendations. *J. Netw. Comput. Appl.* **2020**, *163*, 102663. [\[CrossRef\]](#)
- Verma, P.K.; Verma, R.; Prakash, A.; Agrawal, A.; Naik, K.; Tripathi, R.; Alsabaan, M.; Khalifa, T.; Abdelkader, T.; Abogharaf, A. Machine-to-Machine (M2M) communications: A survey. *J. Netw. Comput. Appl.* **2016**, *66*, 83–105. [\[CrossRef\]](#)
- Tian, L.; Santi, S.; Seferagić, A.; Lan, J.; Famaey, J. Wi-Fi HaLow for the Internet of Things: An up-to-date survey on IEEE 802.11ah research. *J. Netw. Comput. Appl.* **2021**, *182*, 103036. [\[CrossRef\]](#)
- IEEE 802.11ah-2016; Standard for Information Technology—Telecommunications and Information Exchange between Systems—Local and Metropolitan Area Networks—Specific Requirements—Part 11: Wireless LAN Medium Access Control (MAC) and Physical Layer (PHY) Specifications Amendment 2: Sub 1 GHz License Exempt Operation. IEEE: Piscataway, NY, USA, 2017; pp. 1–594. [\[CrossRef\]](#)
- Khorov, E.; Lyakhov, A.; Krotov, A.; Guschin, A. A survey on IEEE 802.11ah: An enabling networking technology for smart cities. *Comput. Commun.* **2015**, *58*, 53–69. [\[CrossRef\]](#)
- Bianchi, G. Performance analysis of the IEEE 802.11 distributed coordination function. *IEEE J. Sel. Areas Commun.* **2000**, *18*, 535–547. [\[CrossRef\]](#)
- Taramit, H.; Barbosa, L.O.; Haqiq, A. Energy Efficiency Framework for Time-limited Contention in the IEEE 802.11ah Standard. In Proceedings of the 2021 IEEE Globecom Workshops (GC Wkshps), Madrid, Spain, 7–11 December 2021; pp. 1–6. [\[CrossRef\]](#)
- Yang, Z.; Ghubaish, A.; Unal, D.; Jain, R. Factors Affecting the Performance of Sub-1 GHz IoT Wireless Networks. *Wirel. Commun. Mob. Comput.* **2021**, 2021. [\[CrossRef\]](#)
- Liao, R.F.; Wen, H.; Wu, J.; Song, H.; Pan, F.; Dong, L. The Rayleigh fading channel prediction via deep learning. *Wirel. Commun. Mob. Comput.* **2018**, 2018, 6497340. [\[CrossRef\]](#)
- Ahmed, N.; Rahman, H.; Hussain, M.I. A comparison of 802.11ah and 802.15.4 for IoT. *ICT Express* **2016**, *2*, 100–102. [\[CrossRef\]](#)
- Domazetović, B.; Kočan, E.; Mihovska, A. Performance evaluation of IEEE 802.11ah systems. In Proceedings of the 2016 24th Telecommunications Forum (TELFOR), Belgrade, Serbia, 22–23 November 2016; pp. 1–4. [\[CrossRef\]](#)
- Banos Gonzalez, V.; Afaqui, M.S.; López Aguilera, E.; García Villegas, E. IEEE 802.11ah: A Technology to Face the IoT Challenge. *Sensors* **2016**, *16*, 1960. [\[CrossRef\]](#)
- Šljivo, A.; Kerkhove, D.; Tian, L.; Famaey, J.; Munteanu, A.; Moerman, I.; Hoebeke, J.; De Poorter, E. Performance Evaluation of IEEE 802.11ah Networks With High-Throughput Bidirectional Traffic. *Sensors* **2018**, *18*, 325. [\[CrossRef\]](#)
- Raeesi, O.; Pirskanen, J.; Hazmi, A.; Levanen, T.; Valkama, M. Performance evaluation of IEEE 802.11ah and its restricted access window mechanism. In Proceedings of the 2014 IEEE International Conference on Communications Workshops (ICC), Sydney, Australia, 10–14 June 2014; pp. 460–466. [\[CrossRef\]](#)
- Santi, S.; Tian, L.; Khorov, E.; Famaey, J. Accurate Energy Modeling and Characterization of IEEE 802.11ah RAW and TWT. *Sensors* **2019**, *19*, 2614. [\[CrossRef\]](#) [\[PubMed\]](#)
- Zazhigina, E.; Yusupov, R.; Khorov, E.; Lyakhov, A. Analytical Study of Periodic Restricted Access Window Mechanism for Short Slots. *Electronics* **2021**, *10*, 549. [\[CrossRef\]](#)
- Khorov, E.; Krotov, A.; Lyakhov, A.; Yusupov, R.; Condoluci, M.; Dohler, M.; Akyildiz, I. Enabling the Internet of Things with Wi-Fi halow—Performance evaluation of the restricted access window. *IEEE Access* **2019**, *7*, 127402–127415. [\[CrossRef\]](#)
- Khorov, E.; Lyakhov, A.; Nasedkin, I.; Yusupov, R.; Famaey, J.; Akyildiz, I.F. Fast and Reliable Alert Delivery in Mission-Critical Wi-Fi HaLow Sensor Networks. *IEEE Access* **2020**, *8*, 14302–14313. [\[CrossRef\]](#)
- Pahlavan, K. *Understanding Communications Networks for Emerging Cybernetics Applications*; River Publishers: Gistrup, Denmark, 2021.
- Daneshgaran, F.; Laddomada, M.; Mesiti, F.; Mondin, M. Unsaturated Throughput Analysis of IEEE 802.11 in Presence of Non Ideal Transmission Channel and Capture Effects. *IEEE Trans. Wirel. Commun.* **2008**, *7*, 1276–1286. [\[CrossRef\]](#)
- Daneshgaran, F.; Laddomada, M.; Mesiti, F.; Mondin, M.; Zanolio, M. Saturation throughput analysis of IEEE 802.11 in the presence of non ideal transmission channel and capture effects. *IEEE Trans. Commun.* **2008**, *56*, 1178–1188. [\[CrossRef\]](#)
- Sutton, G.J.; Liu, R.P.; Collings, I.B. Modelling IEEE 802.11 DCF Heterogeneous Networks with Rayleigh Fading and Capture. *IEEE Trans. Commun.* **2013**, *61*, 3336–3348. [\[CrossRef\]](#)
- Gallager, R.G. *Stochastic Processes: Theory for Applications*; Cambridge University Press: Cambridge, UK, 2013.



- 
24. Ling, X.; Cheng, Y.; Mark, J.W.; Shen, X. A renewal theory based analytical model for the contention access period of IEEE 802.15.4 MAC. *IEEE Trans. Wirel. Commun.* **2008**, *7*, 2340–2349. [[CrossRef](#)]
  25. Zhang, X. A new method for analyzing nonsaturated IEEE 802.11 DCF networks. *IEEE Wirel. Commun. Lett.* **2013**, *2*, 243–246. [[CrossRef](#)]
  26. Khairy, S.; Han, M.; Cai, L.X.; Cheng, Y.; Han, Z. A renewal theory based analytical model for multi-channel random access in IEEE 802.11 ac/ax. *IEEE Trans. Mob. Comput.* **2019**, *18*, 1000–1013. [[CrossRef](#)]
  27. Cocco, D.; Giona, M. Generalized Counting Processes in a Stochastic Environment. *Mathematics* **2021**, *9*, 2573. [[CrossRef](#)]
  28. Goldsmith, A. *Wireless Communications*; Cambridge University Press: Cambridge, UK, 2005.
  29. Zheng, L.; Ni, M.; Cai, L.; Pan, J.; Ghosh, C.; Doppler, K. Performance Analysis of Group-Synchronized DCF for Dense IEEE 802.11 Networks. *IEEE Trans. Wirel. Commun.* **2014**, *13*, 6180–6192. [[CrossRef](#)]
  30. Tian, L.; Lopez-Aguilera, E.; Garcia-Villegas, E.; Mehari, M.T.; De Poorter, E.; Latré, S.; Famaey, J. Optimization-Oriented RAW Modeling of IEEE 802.11ah Heterogeneous Networks. *IEEE Internet Things J.* **2019**, *6*, 10597–10609. [[CrossRef](#)]